Aquaporin-2 trafficking is regulated by PDZ-domain containing protein SPA-1 ☆

Yumi Noda[a,b,*], Saburo Horikawa[c], Tetsushi Furukawa[d], Keiji Hirai[b], Yoshifumi Katayama[b], Tomoki Asai[a], Michio Kuwahara[a], Koko Katagiri[e], Tatsuo Kinashi[e], Masakazu Hattori[f], Nagahiro Minato[f], Sei Sasaki[a]

[a] *Department of Homeostasis Medicine and Nephrology, Graduate School, Tokyo Medical and Dental University, 1-5-45 Yushima, Bunkyo-ku, Tokyo 113-8519, Japan*
[b] *Autonomic Physiology, Tokyo Medical and Dental University, Tokyo 113-8519, Japan*
[c] *Pathological Biochemistry, Tokyo Medical and Dental University, Tokyo 113-8519, Japan*
[d] *Bio-informational Pharmacology, Tokyo Medical and Dental University, Tokyo 113-8519, Japan*
[e] *Departments of Molecular Immunology and Allergy, Kyoto University, Kyoto 606-8501, Japan*
[f] *Immunology and Cell Biology, Kyoto University, Kyoto 606-8501, Japan*

Received 21 April 2004; accepted 10 May 2004

Available online 25 May 2004

Edited by Felix Wieland

Abstract Targeted positioning of water channel aquaporin-2 (AQP2) strictly regulates body water homeostasis. Trafficking of AQP2 to the apical membrane is critical to the reabsorption of water in renal collecting ducts. Controlled apical positioning of AQP2 suggests the existence of proteins that interact with AQP2. A biochemical search for AQP2-interacting proteins led to the identification of PDZ-domain containing protein, signal-induced proliferation-associated gene-1 (SPA-1) which is a GTPase-activating protein (GAP) for Rap1. The distribution of SPA-1 coincided with that of AQP2 in renal collecting ducts. The site of colocalization was concomitantly relocated by hydration status. AQP2 trafficking to the apical membrane was inhibited by the SPA-1 mutant lacking Rap1GAP activity and by the constitutively active mutant of Rap1. AQP2 trafficking was impaired in SPA-1-deficient mice. Our results show that SPA-1 directly binds to AQP2 and regulates at least in part AQP2 trafficking.

Keywords: Aquaporin-2; Trafficking; PDZ protein

1. Introduction

Body water homeostasis is essential for survival of mammals. Water transport occurs through specialized channels called aquaporins (AQPs). AQPs play an important role in reabsorption of water and in concentration of urine in the kidney. At least seven different AQPs exist in the kidney, however, AQP2 is the only known water channel to be regulated by antidiuretic hormone vasopressin [1,2]. The vasopressin tightly regulates body water balance. The binding of vasopressin to vasopressin V2 receptors on renal principal cells stimulates cAMP synthesis via activation of adenylate cyclase. The subsequent activation of protein kinase A (PKA) leads to phosphorylation of AQP2 and this phosphorylation event is required to increase the water permeability and water reabsorption of principal cells. In this process, subapical storage vesicles in principal cells containing AQP2 translocate to and fuse with the apical plasma membrane, rendering the cell water permeable. Upon removal of vasopressin, AQP2 is internalized by endocytosis into the storage vesicles that restore the water-impermeable state of the cell. However, the molecular mechanism by which PKA phosphorylation of AQP2 facilitates this transport process is unclear.

Controlled apical positioning of AQP2 suggests the existence of proteins that recruit AQP2 by binding directly. To date, several proteins which are localized in AQP2-bearing vesicles and are supposed to mediate its sorting and exocytic insertion have been reported (e.g., Rab proteins, soluble NSF attachment protein receptors (SNAREs), and cytoskeletal proteins) [1], however, proteins that directly interact with AQP2 and provide specificity in AQP2 sorting have not yet been identified.

Mutations in human AQP2 or downregulation of AQP2 expression cause hereditary or acquired nephrogenic diabetes insipidus (NDI), a disease characterized by a massive loss of water through the kidney [1]. In addition, AQP2-T126M knock-in mice with impaired AQP2 trafficking have severe NDI with neonatal mortality [3]. Recently, AQP2 mutations with dominant-type NDI showed the importance of C terminus of AQP2 for its trafficking [4–6]. Interestingly, the C-terminal sequences of human, mouse and rat AQP2 (Gly–Thr/Ser–Lys–Ala) match to the class I PDZ-interacting motif (X–Thr/Ser–X–Φ) (X, unspecified amino acid; Φ, hydrophobic amino acid) [7]. It is well known that PDZ-domain containing proteins are involved in targeting, anchoring, and stabilizing of membrane proteins. Therefore, we speculated the existence of the proteins that interacted with AQP2 through a PDZ-domain interaction.

☆ Data deposition: GenBank Accession No. for the cDNA sequence reported in this paper is AB091474.

* Corresponding author. Fax: +81-3-5803-5215.
E-mail address: ynodmed2@tmd.ac.jp (Y. Noda).

Abbreviations: AQP2, aquaporin-2; MDCK cells, Madin–Darby canine kidney cells; NDI, nephrogenic diabetes insipidus

0014-5793/$22.00
doi:10.1016/j.febslet.2004.05.021

In this study, we identified the PDZ-domain containing protein which directly bound to AQP2 and regulated AQP2 trafficking.

2. Materials and methods

2.1. Pull-down experiments

PDZ1 domain (amino acid residues (aa) 1–98) and PDZ2 domain (aa 139–248) of EBP50 [8], the N-terminal region (aa 1–610), PDZ domain (aa 685–760) and C-terminal region (aa 844–1040) of rat signal-induced proliferation-associated gene-1 (SPA-1) were subcloned into pGEX-4T-1 (Amersham) to generate GST-fusion proteins. C-terminal region of human AQP2 (aa 226–271 (AQP2CT)) was subcloned into pQE40 (Qiagen) to generate dihydrofolate reductase (DHFR)-fusion protein. DHFR was fused to the N-terminus of AQP2CT. To generate AQP2CT(AAAA), the last four amino acids of AQP2CT were substituted with four alanine residues. GST-fusion proteins were expressed in *Escherichia coli* BL21(DE3). Each protein (5 μg) was immobilized on glutathione–Sepharose (Amersham) and was combined with solubilized AQP2CT/DHFR proteins (10 μg) or AQP2CT(AAAA)/DHFR proteins (10 μg) prepared from *E. coli* M15(pREP4). Bound proteins were eluted by glutathione and analyzed by Western blotting with an affinity-purified rabbit antibody against C terminus of AQP2 [9].

2.2. Immunoscreening of cDNA library form rat kidney papilla

All animal experiments in this study were approved by the Institutional Animal Care and Use Comittee of Tokyo Medical and Dental University. Rat kidney papilla mRNA was isolated using mRNA purification kit (Amersham), and a cDNA expression library was constructed in λTripleEx2 vector using cDNA library construction kit (Clontech). Immunoscreening was performed using anti-PDZ1-EBP50 antibody [10] as described [11].

2.3. Immunoblot analysis of SPA-1

Tissues from rat kidney cortex and papilla were homogenized in a solution containing 50 mM Tris–HCl, pH 7.4, 1 mM 2-mercaptoethanol, and 1 mM EDTA. Madin–Darby canine kidney (MDCK) cells were solubilized in lysis buffer containing 20 mM Tris–HCl, pH 7.4, 150 mM NaCl, and 1% NP-40. Each sample was analyzed by Western blotting with anti-SPA-1 antibody [12].

2.4. Immunoprecipitation

Rat kidney papillae were homogenized in lysis buffer containing 20 mM Tris–HCl, pH 7.5, 150 mM NaCl, 0.5% Tween 20, 100 mM 3-isobutyl-1-methylxanthine, 10 mM β-glycerophosphate, 0.15 mM sodium orthovanadate, 1 mM dithiothreitol, and an EDTA-free protease inhibitor mixture (Roche). The homogenates were spun at $20\,000 \times g$ for 30 min and 500 μl (500 μg protein) of the supernatants were incubated with anti-SPA-1 antibody or anti-AQP2 antibody. Immunocomplex was precipitated with protein A–Sepharose and

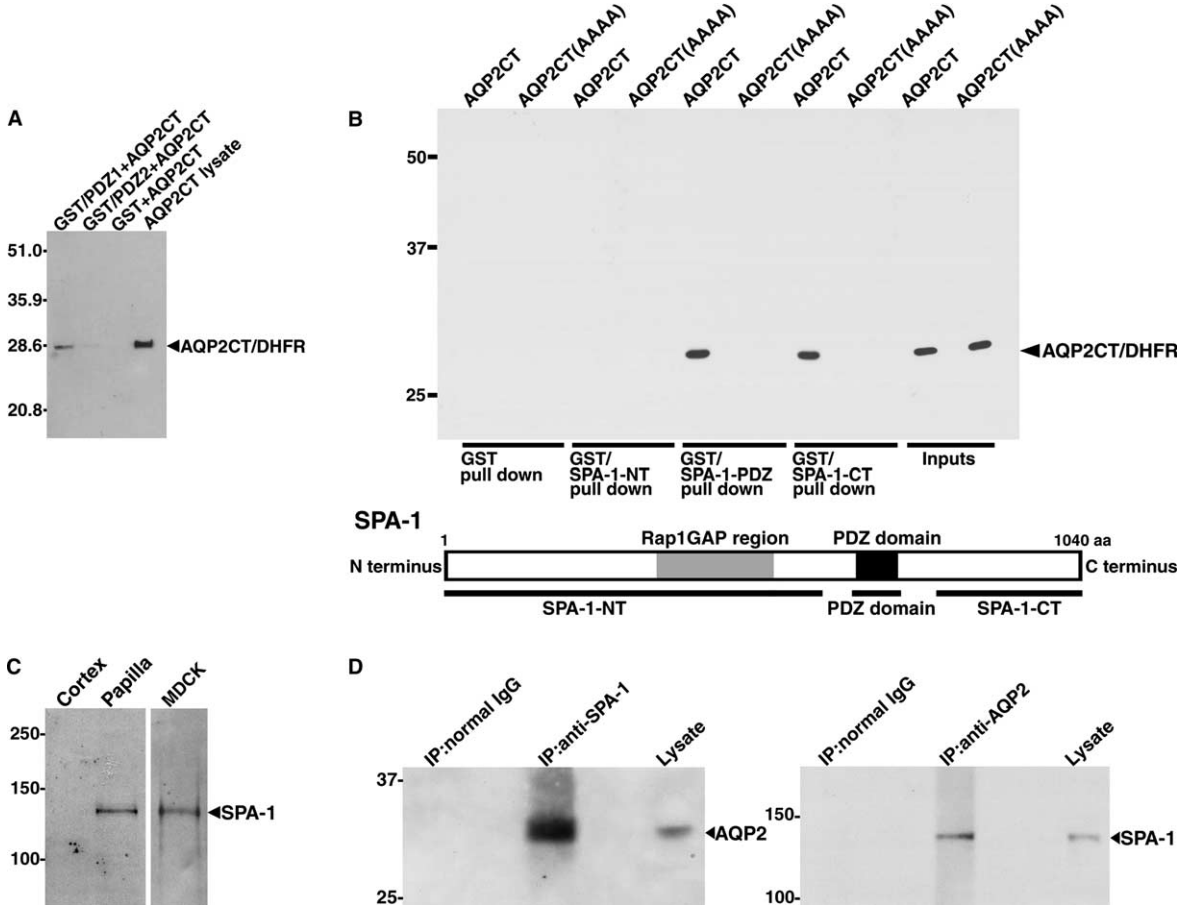

Fig. 1. SPA-1 binding to AQP2. (A) Pull-down assays. AQP2CT/DHFR was pulled down using each GST/PDZ1 and GST/PDZ2 of EBP50. Bound proteins were immunoblotted with anti-AQP2 antibody. The molecular mass of AQP2CT/DHFR is 28.6 kDa. Molecular mass standards (in kDa) were indicated on the left. (B) Pull-down assays using GST/SPA-1-NT, GST/SPA-1-PDZ and GST/SPA-1-CT, respectively. Anti-AQP2 antibody recognized equally both wild-type (AQP2CT) and mutant proteins (AQP2CT(AAAA)) (input control lysate lanes). Schematic representation of SPA-1-NT, SPA-1-PDZ and SPA-1-CT is shown in under part. (C) Immunoblot analysis of SPA-1 in rat kidney cortex, papilla, and MDCK cells. Tissue extracts were immunoblotted with anti-SPA-1 antibody. (D) Coimmunoprecipitation experiments of SPA-1 and AQP2. Extracts of rat kidney papillae were immunoprecipitated with anti-SPA-1 antibody, anti-AQP2 antibody or normal IgG. Precipitates were immunoblotted for AQP2 (left panel) and SPA-1 (right panel), respectively. Inputs represent 10% of the lysates used for the immunoprecipitation reaction.

eluted by boiling in Laemmli buffer. Normal rabbit IgG was used as negative control. Cell extracts (50 μg protein) and immunoprecipitated samples were analyzed by Western blotting with anti-AQP2 or anti-SPA-1 antibody.

2.5. Immunohistochemistry in renal collecting ducts

For double immunolabelling of AQP2 and SPA-1, rat kidney was fixed with 4% paraformaldehyde in PBS, cryoprotected with 20% sucrose in PBS, embedded in OCT compound, and frozen in liquid N_2. Cryostat sections were blocked with 3% goat serum in PBS and incubated with anti-SPA-1 antibody followed by incubation with Alexa 488 anti-rabbit IgG (Molecular Probes). The sections were washed and incubated with unlabelled goat anti-rabbit IgG. After washing, sections were incubated with anti-AQP2 antibody followed by incubation with Alexa 546 anti-rabbit IgG. Immunofluorescence images were viewed with LSM 510 confocal microscope (Carl Zeiss). Control experiments were performed with non-immune IgG for each primary antibody, revealing no positive staining.

For immunolabelling of AQP2 in kidneys from SPA-1-deficient mice [13,14] and wild-type mice, the samples were stained by anti-AQP2 antibody and visualized by Alexa 488 anti-rabbit IgG.

2.6. Quantitative immunofluorescence

To quantify the distribution of AQP2 and SPA-1 in collecting duct cells, the immunofluorescence intensities were analyzed using Scion Image (Scion Corporation). At least three different fields of the coverslips were analyzed from two separate experiments for each group. In each cell, the cytoplasmic area was marked on the differential-interference-contrast light micrographs. The distribution of pixel intensity in the cytoplasmic area of each cell was determined by the software and skewness was calculated. Skewness is a measure of symmetry of a profile about the mean pixel intensity.

2.7. Transfection and cell surface labelling of AQP2

LIG–SPA-1 mutant, which lacked Rap1GAP activity [15,16], was generated by mutating RKR residues (aa 420–422) of SPA-1 to LIG using site-direct mutagenesis kit (Stratagene). Flag epitope tag was introduced at the N-terminal end of the mutant. Rap1 mutants were produced from the corresponding cDNA by replacement of glycine with valine at position 12 (Rap1V12) and by substitution of serine for asparagine at position 17 (Rap1N17), respectively. T7 epitope tag was introduced at the N-terminal end of each mutant. The constructs were subcloned in pcDL-SRa296.

MDCK cells stably expressing AQP2 proteins (MDCK/AQP2) [17] were cultured in DMEM supplemented with 10% fetal bovine serum, 100 U/ml of penicillin, 100 μg/ml of streptomycin, and 700 μg/ml of G418 (Sigma). The cells grown on permeable filter supports (Corning) were transiently transfected with these mutants using LipofectAMINE 2000 (Invitrogen). The cells were stimulated with 40 nM forskolin for 30 min. In Rap1N17 transfected cells, H89 (final concentration 30 μM; Seikagaku Corporation, Tokyo) was added to the medium for 30 min before the forskolin treatment. The cells were fixed with 4% paraformaldehyde, blocked with 1% BSA in PBS, incubated with rabbit antibody against the external C-loop of AQP2 raised using an oligopeptide (aa 113–127) [2], and incubated with Alexa 488 anti-rabbit IgG antibody. The cells were then permeabilized with 0.1% Triton X-100 and blocked with 2% BSA and 10% goat serum in PBS. The cells transfected with LIG–SPA-1 were incubated with anti-Flag M2 antibody (Sigma), and the cells transfected with Rap1V12 and Rap1N17 were incubated with anti-T7 antibody (Novagen), respectively. The cells in each experiment were then incubated with Alexa 568 anti-mouse IgG antibody.

2.8. Adenovirus-mediated Rap1V12 expression and immunolabelling for surface-localized AQP2

MDCK/AQP2 cells were infected with adeno/GFP-Rap1V12 [18]. The cells were treated with 40 nM forskolin for 30 min and fixed with 4% paraformaldehyde. Apical localized AQP2 was immunolabelled as described above and visualized with Alexa 546 anti-rabbit IgG antibody. For double immunolabelling of AQP2 and Na^+/K^+-ATPase, the cells were treated with 0.1% Triton X-100 and incubated with rabbit antibody against C-terminus of AQP2 followed by incubation with Alexa 488 anti-rabbit IgG antibody. After washing, sections were incubated with chicken antibody against canine Na^+/K^+-ATPase (Abcam) and then with Alexa 594 anti-chicken IgG antibody.

2.9. Cell surface biotinylation

Apical cell surface labelling was performed as described [19] except the lysis buffer (150 mM NaCl, 50 mM Tris–HCl, pH 7.5, 5 mM EDTA, 1% NP-40, 0.1% SDS, 0.5% deoxycholate and protease inhibitor mixture). Quantification of the bands was performed using Scion Image.

2.10. Statistical analyses

Statistical analyses were made using unpaired Student's t test. Differences were considered significant at P value less than 0.05.

3. Results

3.1. Identification of AQP2-binding protein

To examine whether the C-terminus of AQP2 (AQP2CT) interacts with PDZ domains, we performed pull-down assays using GST-fusion proteins containing either of the two PDZ domains of EBP50, an epithelium-specific scaffolding protein [8]: PDZ1 (aa 1–98) or PDZ2 (aa 139–248) (Fig. 1A). AQP2CT

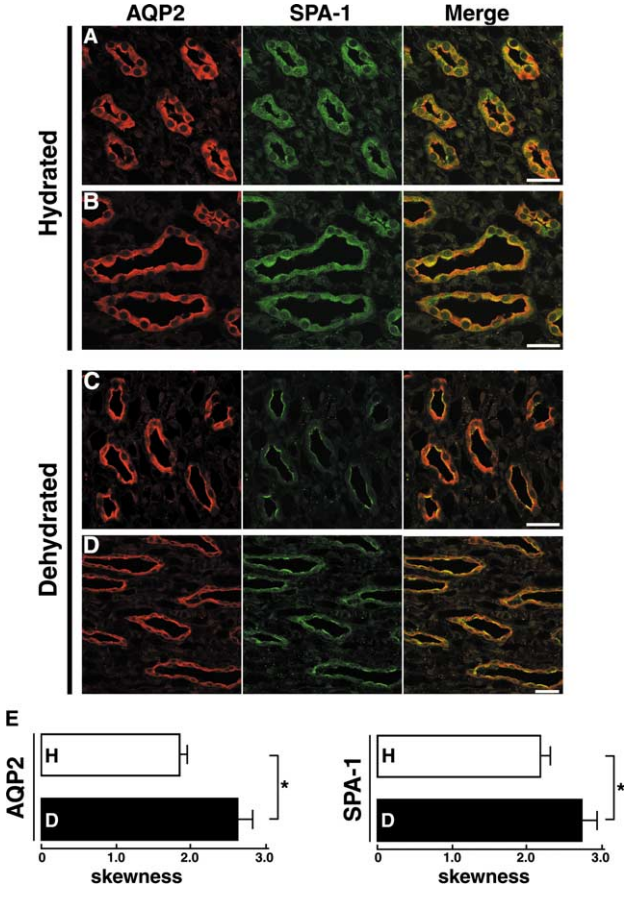

Fig. 2. Localization of AQP2 and SPA-1 in renal collecting ducts. Rats were hydrated (A,B) or water-deprived (C,D) for 24 h. (A,C) Transverse sections; (B,D) longitudinal sections through collecting duct tubules. Left panels, immunolabelling of AQP2 (red); middle panels, immunolabelling of SPA-1 (green); right panels, merged images of AQP2 and SPA-1. Yellow indicates colocalization of AQP2 and SPA-1. Scale bars: 50 μm. (E) Quantitative analyses for the translocation of AQP2 and SPA-1 induced by dehydration. From the immunofluorescence distributions of AQP2 and SPA-1 as shown above, the statistical parameter of skewness was calculated. White bars (H) indicate the values under hydrated conditions and black bars (D) indicate the values under dehydrated conditions. Data represent means and S.E. from 20 cells of two independent experiments. *$P < 0.05$.

bound strongly to GST/PDZ1 and faintly to GST/PDZ2, but did not bind to GST alone, indicating that AQP2 might interact with proteins containing a PDZ1-like sequence. To isolate such proteins, we performed an immunoscreening of rat kidney papilla cDNA expression library using antibody against PDZ1 domain, because AQP2 was expressed abundantly in papilla [2]. From 1.4×10^6 independent recombinants, three positive clones were isolated. These clones encoded partial polypeptide fragments derived from the same protein. The deduced amino acid sequence from the complete nucleotide sequence encoded a polypeptide of 1040-amino acids. The protein shows extremely high overall homology to mouse SPA-1 (96%) and to human SPA-1 (89%), respectively [12]. These findings indicate that the protein deduced from our cDNA is the rat counterpart of SPA-1. To examine whether SPA-1 binds specifically to the C-terminus of AQP2 (AQP2CT), we performed pull-down assays using N-terminal region (aa 1–610: SPA-1-NT), PDZ domain (aa 685–760: SPA-1-PDZ) and C-terminal region (aa 844–1040: SPA-1-CT) of SPA-1 expressed as GST-fusion proteins (Fig. 1B). Both GST/SPA-1-PDZ and GST/SPA-1-CT interacted with AQP2CT. GST/SPA-1-NT and GST alone did not bind to AQP2CT. In contrast to SPA-1-PDZ, SPA-1-CT did not contain a typical sequence of PDZ domain. It is supposed that SPA-1-CT may mimic a conformational similarity to a PDZ domain. Substitution of the last four amino acids of AQP2CT with four alanine residues (AQP2CT(AAAA)) abrogated these two interactions. This finding shows the significance of the C-terminus of AQP2 for the interaction with SPA-1.

To examine the existence of SPA-1 in the kidney, immunoblots were performed using tissue extracts from rat kidney cortex and papilla, respectively (Fig. 1C left panel). SPA-1 was obviously detected in papilla and faintly in cortex. SPA-1 was also detected in cultured MDCK cells (Fig. 1C, right panel).

To verify the endogenous interaction of SPA-1 and AQP2 in the kidney papilla, we performed coimmunoprecipitation assays (Fig. 1D). From the tissue extracts of rat papilla, AQP2 was coimmunoprecipitated with anti-SPA-1 antibody and SPA-1 was also coimmunoprecipitated with anti-AQP2 antibody, respectively. On the contrary, AQP2 and SPA-1 were not immunoprecipitated with normal IgG. Coimmunoprecipitation analysis showed that endogenous AQP2 and SPA-1 proteins formed a complex in the kidney papilla.

3.2. SPA-1 colocalizes with AQP2 in renal collecting ducts

To examine whether SPA-1 controls AQP2 sorting, we performed immunohistochemistry for SPA-1 and AQP2 in the kidney papilla (Fig. 2). In hydrated rats, AQP2 was localized predominantly in the intracellular vesicles of renal collecting duct principal cells (Fig. 2A and B, left panels). Water deprivation accumulated AQP2 in the apical region of the cells (Fig. 2C and D, left panels). The distribution of SPA-1 was also changed by water balance alteration. In hydrated rats, SPA-1 was localized predominantly in the intracellular vesicles (Fig. 2A and B, middle panels). Water-deprivation increased the accumulation of SPA-1 labelling in the apical region (Fig. 2C and D, middle panels). Double immunolabelling of AQP2 and SPA-1 revealed colocalization of the two proteins in the apical region of collecting duct cells upon water-deprivation and in the intracellular vesicles upon hydration, respectively (Fig. 2A–D, right panels). These findings strongly suggest that AQP2 and SPA-1 are simultaneously regulated by water balance and SPA-1 may be involved in recruitment of AQP2 to the targeted site.

To confirm the translocation of the two proteins quantitatively, we calculated skewness of these signal intensity distributions (Fig. 2E). A random pixel intensity distribution is characterized by a low value in skewness, whereas most pixels concentrated in a narrow range are characterized by a high value in skewness. Under hydrated conditions AQP2 was distributed randomly and skewness was 1.84 ± 0.11, whereas under dehydrated conditions the value significantly increased

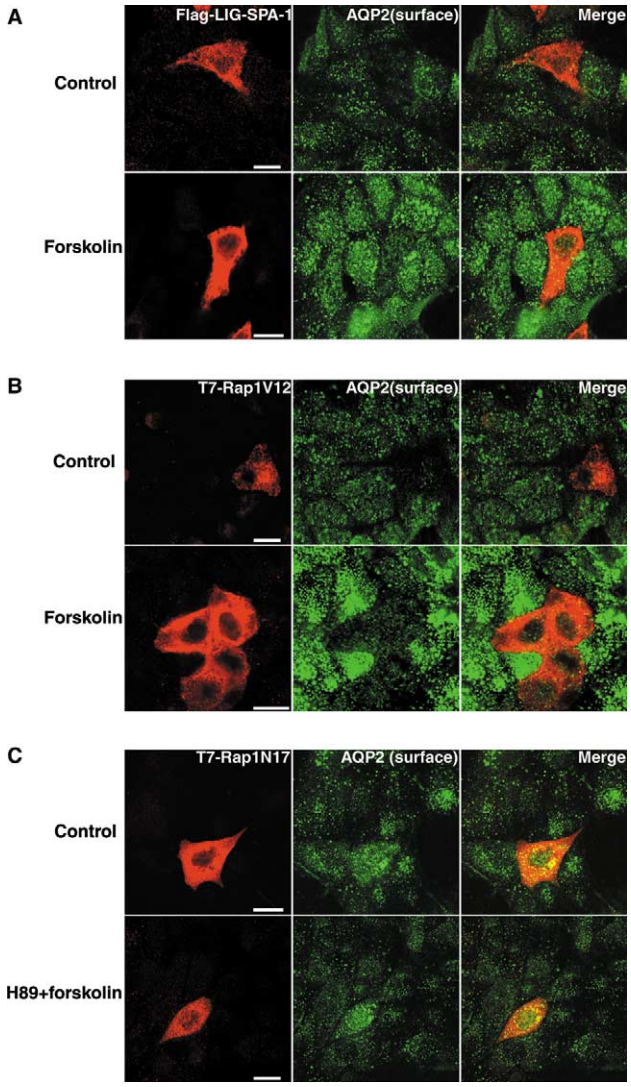

Fig. 3. Surface labelling for AQP2 in each LIG–SPA-1, Rap1V12, and Rap1N17-transfected MDCK/AQP2 cells. (A) MDCK/AQP2 cells transfected with Flag-LIG–SPA-1 were treated without (upper panels) or with (lower panels) forskolin. The cells were double-labelled for Flag-LIG–SPA-1 (left panels, red) and surface-localized AQP2 (middle panels, green), and merged in right panels. (B) MDCK/AQP2 cells transfected with T7-Rap1V12 were treated without (upper panels) or with (lower panels) forskolin. The cells were double-labelled for T7-Rap1V12 (left panels, red) and surface-localized AQP2 (middle panels, green), and merged in right panels. (C) MDCK/AQP2 cells transfected with T7-Rap1N17 were left untreated (upper panels) or pretreated with H89, a PKA inhibitor, before incubation with forskolin (lower panels). The cells were double-labelled for T7-Rap1N17 (left panels, red) and surface-localized AQP2 (middle panels, green), and merged in right panels. Scale bars: 10 μm.

(2.62 ± 0.20, $P < 0.05$). Water-deprivation also increased significantly the value of SPA-1 distribution compared to that under hydrated conditions (2.72 ± 0.21 versus 2.18 ± 0.13, $P < 0.05$). These results indicate that SPA-1 is relocated by hydration status in a manner similar to AQP2 translocation.

3.3. AQP2 trafficking is regulated by Rap1 signalling

SPA-1 is a GTPase-activating protein (GAP) for Rap1 and inactivates Rap1 [12]. To assess the role of SPA-1 in AQP2 trafficking, we examined the effect of dominant-negative mutant LIG–SPA-1 which lacked GAP activity on AQP2 localization in the MDCK/AQP2 cells [17] (Fig. 3A). In the cells transfected with LIG–SPA-1 (red), cell surface labelling of AQP2 was decreased as compared to the untransfected cells under the basal condition. Forskolin treatment increased AQP2 translocation to the cell surface in the untransfected cells, however, the surface delivery of AQP2 was still inhibited by this treatment in the mutant transfected cells. These findings show that GAP activity of SPA-1 is important for AQP2 trafficking.

Next, we examined the contribution of Rap1 signalling to AQP2 trafficking. In the cells transfected with Rap1V12 (red), which was a constitutively active mutant, the surface expression of AQP2 was also decreased as compared to the untransfected cells with or without forskolin stimulation (Fig. 3B). These findings show that increase in active form of Rap1 impairs the surface delivery of AQP2.

On the other hand, in the cells transfected with dominant negative mutant Rap1N17 (red), the cell surface labelling of AQP2 increased as compared to the untransfected cells (Fig. 3C). Pretreatment with H89, a specific PKA inhibitor, abolished the forskolin-induced translocation of AQP2 in the untransfected cells, however, the highly positive signals of cell surface labelling of AQP2 were observed in Rap1N17 trans-

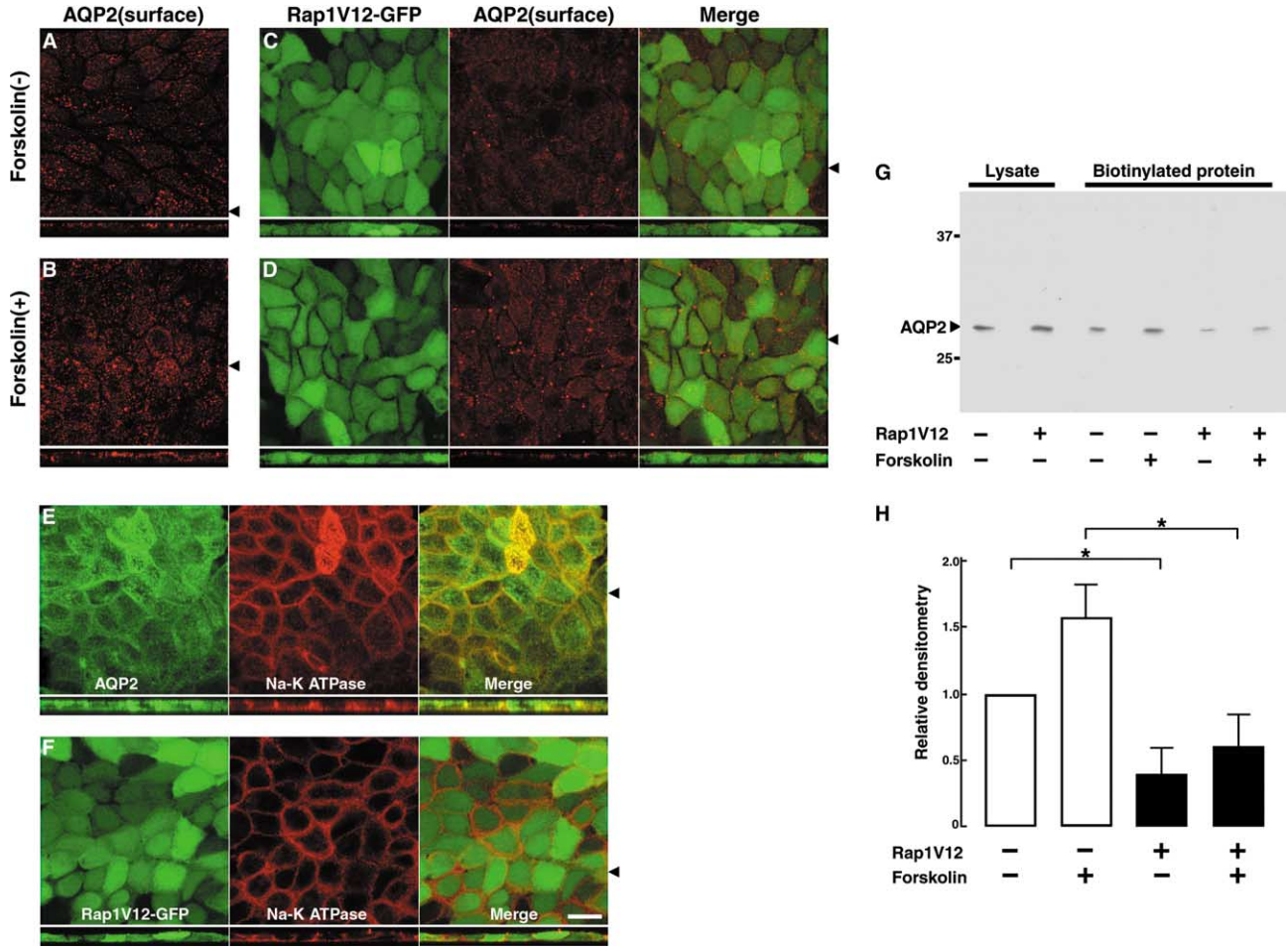

Fig. 4. Rap1V12 inhibits AQP2 translocation to the apical membrane. (A–D) MDCK/AQP2 cells either expressing GFP-Rap1V12 (C,D) or not (A,B) were treated without (A,C) or with (B,D) forskolin and were labelled for surface-localized AQP2 (red). Right panels of C and D show green fluorescence for GFP-Rap1V12, middle panels show red for surface-localized AQP2, and left panels show the overlay images. The *xy* planes show sections from apical surface of the cells and each lower strip represents *xz* scan at the position indicated by the black arrowhead on the right. *xz* scan shows distribution of red fluorescence for apical-localized AQP2 along the upper surface (apical membrane). (E) MDCK/AQP2 cells were double-labelled with antibody against C terminus of AQP2 (left panel, green) and anti-Na^+/K^+-ATPase antibody (middle panel, red), and merged in right panel. (F) MDCK/AQP2 cells expressing GFP-Rap1V12 (green, left panel) were labelled for Na^+/K^+-ATPase (middle panel, red). Right panel shows the overlay image. Scale bar in F is 10 μm that is applied to other panels. (G) MDCK/AQP2 cells either expressing GFP-Rap1V12 or not as described above were subjected to a cell surface biotinylation assay. Biotinylated proteins were precipitated with streptavidin-agarose beads and immunoblotted for AQP2. (H) Summary of quantitative densitometry expressed as averaged relative levels normalized to 1.0 for non-transfected MDCK/AQP2 cells without forskolin incubation. Data represent means and S.E. from three independent experiments. *$P < 0.05$.

fected cells. This finding shows that Rap1N17 suppresses the endogenous Rap1 activity and increases the AQP2 trafficking to the cell surface.

To confirm the role of Rap1 signalling in AQP2 trafficking, we used adenovirus vector for efficient and homogeneous expression of Rap1V12 (Fig. 4). Under the basal condition, apical labelling of AQP2 in Rap1V12-expressing cells was decreased as compared to the control cells (Fig. 4A and C). Although forskolin treatment increased AQP2 translocation to the apical membrane in the control cells, the apical delivery of AQP2 was still inhibited by this treatment in Rap1V12-expressing cells (Fig. 4B and D). The staining pattern of a basolateral marker, Na^+/K^+-ATPase was not changed by Rap1V12, indicating that Rap1V12 did not affect the cell polarity (Fig. 4E and F). To quantify the effect of Rap1V12 on the AQP2 translocation to the apical surface, a cell surface biotinylation assay was performed (Fig. 4G and H). Expression of Rap1V12 did not alter the total amount of AQP2 in the cells. Apical localized AQP2 in Rap1V12-expressing cells under the basal conditions was significantly decreased compared to that in the control cells (0.38 ± 0.20 versus 1, $P < 0.05$). Under forskolin stimulation, apical expression of AQP2 was also decreased significantly compared to that in the control cells (0.59 ± 0.24 versus 1.57 ± 0.25, $P < 0.05$). These results confirm that AQP2 trafficking is inhibited by Rap1 activation.

3.4. SPA-1 deficiency impairs AQP2 trafficking

To examine the contribution of SPA-1 to the AQP2 trafficking in vivo, we performed immunohistochemistry for AQP2 in renal collecting duct principal cells in SPA-1-deficient mice [13,14] under water-deprivation (Fig. 5A–D). Contrary to the wild-type mice, AQP2 was not restricted to the apical region and diffusely distributed in the cytoplasm in the knockout mice. To quantify the distribution of AQP2, skewness was calculated from the immunofluorescence distribution of AQP2 (Fig. 5E). Skewness value in knockout mice was significantly reduced compared to that in wild-type mice (1.23 ± 0.42 versus 1.79 ± 0.093, $P < 0.001$). These results confirm that AQP2 translocation induced by water-deprivation is impaired in the knockout mice.

4. Discussion

Apical localization of AQP2 carries out water reabsorption in renal collecting ducts. Misrouting of AQP2 is considerably important in the pathophysiology of water balance disorders including NDI. In the present experiments, we have discovered the protein that regulates AQP2 sorting by binding directly.

To date, several proteins involved in AQP2 sorting have been reported [1]. SNARE proteins are involved in the process of docking and fusion of AQP2-containing vesicles to the apical membrane. A complex of dynein and dynactin, which is expected to be involved in the movement of vesicles toward the apical membrane, associates with AQP2-bearing vesicles. In spite of these reports, proteins that directly interact with AQP2 and provide specificity in AQP2 sorting have not yet been clarified.

In this study, we have successfully identified the AQP2-binding protein, SPA-1. Biochemical and histochemical analyses show that SPA-1 directly binds to AQP2 and regulates the trafficking of AQP2 to the apical membrane. It is known that there are several SPA-1-related proteins with similar functions [20,21]. Among these proteins only SPA-1 was isolated from rat kidney papilla cDNA expression library, indicating that SPA-1 might play a major role in AQP2 trafficking in renal collecting ducts. However, we cannot exclude the possibility that SPA-1-related proteins may also be involved in AQP2 trafficking like SPA-1.

SPA-1 is a GAP for Rap1 [12,22]. Rap1 is a Ras-related small GTPase and is implicated in many cellular processes including regulation of Ras/ERK signalling pathway, cell morphogenesis and cell differentiation [20]. Rap1 may also be required for cytoskeletal organization through the crosstalk with other small GTPases, including Ral and Rho [22]. It has been recently reported that Rap1 GTPases are critical for

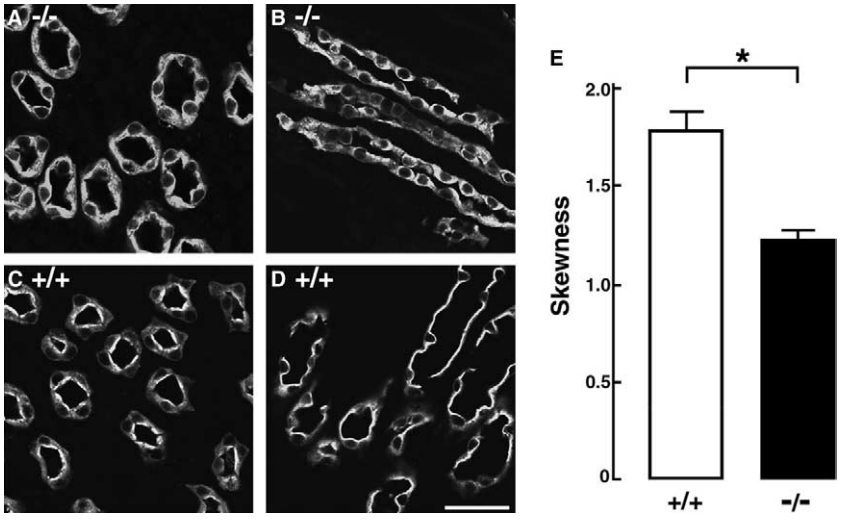

Fig. 5. Localization of AQP2 in the renal medulla of SPA-1-deficient mice under water deprivation. (A,B) SPA-1-deficient mice; (C,D) wild-type mice. (A,C) Transverse sections; (B,D) longitudinal sections through collecting duct tubules. Scale bar: 50 μm. (E) Quantitative analysis for the distribution of AQP2 in SPA-1-deficient mice (−/−) and wild-type mice (+/+). From the immunofluorescence distribution of AQP2 skewness was calculated. Data represent means and S.E. from 40 cells of two independent experiments. *$P < 0.001$ compared with wild-type mice.

vesicle trafficking [23]. These findings support our suggested mechanism that SPA-1, a GAP for Rap1, is involved in membrane protein sorting.

In addition, it is reported that RhoGTP prevents AQP2 translocation to the apical membrane by stimulating F-actin polymerization [24,25]. In the present study, we have shown that GAP activity of SPA-1 is required for AQP2 trafficking. We are tempting to speculate that Rap1 affects the assembly of F-actin that functions as a barrier for the AQP2 trafficking between the apical membrane and the intracellular compartments through the crosstalk with Rho family GTPases. Thus, SPA-1 binding to AQP2 may reduce the levels of Rap1GTP that trigger F-actin disassembly in a restricted area, resulting in the promotion of the AQP2 sorting.

PDZ proteins regulate membrane protein sorting by providing the molecular link between membrane proteins and cytoskeletal elements [7,26]. GAPs for small GTPases are known to be effectors that mediate various signal transduction pathways. According to the benefits of SPA-1 as a PDZ protein and a GAP, SPA-1 may regulate protein trafficking.

In the present experiments, we have discovered the protein that regulates AQP2 sorting by binding directly. Our finding is the first report concerning the interaction between a member of GAPs and a member of recycling channel proteins, providing a wider role for GAPs and a novel mechanism for membrane protein trafficking.

Acknowledgements: We thank Drs. K. Honda, J. Kawagoe and K. Kobayashi, Tokyo Medical and Dental University for helpful advice. This work was supported by grants from the Ministry of Education, Culture, Sports, Science, and Technology of Japan.

References

[1] Nielsen, S., Frøkiaer, J., Marples, D., Kwon, T.H., Agre, P. and Knepper, M.A. (2002) Physiol. Rev. 82, 205–244.
[2] Fushimi, K., Uchida, S., Hara, Y., Hirata, Y., Marumo, F. and Sasaki, S. (1993) Nature 361, 549–552.
[3] Yang, B., Gillespie, A., Carlson, E.J., Epstein, C.J. and Verkman, A.S. (2001) J. Biol. Chem. 276, 2775–2779.
[4] Kamsteeg, E.J., Wormhoudt, T.A.M., Rijss, J.P.L., van Os, C.H. and Deen, P.M. (1999) EMBO J. 18, 2394–2400.
[5] Kuwahara, M., Iwai, K., Ooeda, T., Igarashi, T., Ogawa, E., Katsushima, Y., Shinbo, I., Uchida, S., Terada, Y., Arthus, M.F., Lonergan, M., Fujiwara, T.M., Bichet, D.G., Marumo, F. and Sasaki, S. (2001) Am. J. Hum. Genet. 69, 738–748.
[6] Marr, N., Bichet, D.G., Lonergan, M., Arthus, M.F., Jeck, N., Seyberth, H.W., Rosenthal, W., van Os, C.H., Oksche, A. and Deen, P.M. (2002) Hum. Mol. Genet. 11, 779–789.
[7] Harris, B.Z. and Lim, W.A. (2001) J. Cell Sci. 114, 3219–3231.
[8] Reczek, D., Berryman, M. and Bretscher, A. (1997) J. Cell Biol. 139, 169–179.
[9] Yamashita, Y., Hirai, K., Katayama, Y., Fushimi, K., Sasaki, S. and Marumo, F. (2000) Am. J. Physiol. Renal Physiol. 278, F395–405.
[10] Ogura, T., Furukawa, T., Toyozaki, T., Yamada, K., Zheng, Y.J., Katayama, Y., Nakaya, H. and Inagaki, N. (2002) FASEB J. 16, 863–865.
[11] Sambrook, J., Fritsch, E.F. and Maniatis, T. (1989) Molecular Cloning: A Laboratory Manual, 2nd ed. Cold Spring Harbor Laboratory Press, Cold Spring Harbor, NY.
[12] Kurachi, H., Wada, Y., Tsukamoto, N., Maeda, M., Kubota, H., Hattori, M., Iwai, K. and Minato, N. (1997) J. Biol. Chem. 272, 28081–28088.
[13] Ishida, D., Yang, H., Masuda, K., Uesugi, K., Kawamoto, H., Hattori, M. and Minato, N. (2003) Proc. Natl. Acad. Sci. USA 100, 10919–10924.
[14] Ishida, D., Kometani, K., Yang, H., Kakugawa, K., Masuda, K., Iwai, K., Suzuki, M., Itohara, S., Nakahata, T., Hiai, H., Kawamoto, H., Hattori, M. and Minato, N. (2003) Cancer Cell 4, 55–65.
[15] Reedquist, K.A., Ross, E., Koop, E.A., Wolthuis, R.M., Zwartkruis, F.J., van Kooyk, Y., Salmon, M., Buckley, C.D. and Bos, J.L. (2000) J. Cell Biol. 148, 1151–1158.
[16] Scheffzek, K., Ahmadian, M.R. and Wittinghofer, A. (1998) Trends Biochem. Sci. 23, 257–262.
[17] Asai, T., Kuwahara, M., Kurihara, H., Sakai, T., Terada, Y., Marumo, F. and Sasaki, S. (2003) Kidney Int. 64, 2–10.
[18] Shimonaka, M., Katagiri, K., Nakayama, T., Fujita, N., Tsuruo, T., Yoshie, O. and Kinashi, T. (2003) J. Cell Biol. 161, 417–427.
[19] van Balkom, B.W., Savelkoul, P.J., Markovich, D., Hofman, E., Nielsen, S. and van der Sluijs and Deen, P.M. (2002) J. Biol. Chem. 277, 41473–41479.
[20] Bos, J.L., de Rooij, J. and Reedquist, K.A. (2001) Nat. Rev. Mol. Cell Biol. 2, 369–377.
[21] Roy, B.C., Kohu, K., Matsuura, K., Yanai, H. and Akiyama, T. (2002) Genes Cells 7, 607–617.
[22] Tsukamoto, N., Hattori, M., Yang, H., Bos, J.L. and Minato, N. (1999) J. Biol. Chem. 274, 18463–18469.
[23] Moskalenko, S., Henry, D.O., Rosse, C., Mirey, G., Camonis, J.H. and White, M.A. (2002) Nat. Cell Biol. 4, 66–72.
[24] Klussmann, E., Tamma, G., Lorenz, D., Wiesner, B., Maric, K., Hofmann, F., Aktories, K., Valenti, G. and Rosenthal, W. (2001) J. Biol. Chem. 276, 20451–20457.
[25] Tamma, G., Klussmann, E., Maric, K., Aktories, K., Svelto, M., Rosenthal, W. and Valenti, G. (2001) Am. J. Physiol. Renal Physiol. 281, F1092–1101.
[26] Sheng, M. and Sala, C. (2001) Annu. Rev. Neurosci. 24, 1–29.